

Hot isostatic pressing of tetragonal ZrO_2 solid-solution powders prepared from acetylacetonates in the system ZrO_2 – Y_2O_3 – Al_2O_3

H. WATANABE, K. HIROTA, O. YAMAGUCHI*

Department of Applied Chemistry, Faculty of Engineering, Doshisha University, Kyoto 602, Japan

S. INAMURA, H. MIYAMOTO

Osaka Prefectural Institute of Industrial Technology, Osaka 550, Japan

N. SHIOKAWA, K. TSUJI

Osaka Cement Co. Ltd, Osaka 597, Japan

In compositions having $ZrO_2/Y_2O_3 = (74.25-71.25)/(0.75-3.75)$ (mol % ratio) with 25 mol % Al_2O_3 , metastable *t*- ZrO_2 solid solutions crystallize at $\sim 780^\circ$ to $\sim 860^\circ$ C from amorphous materials prepared by the simultaneous hydrolysis of zirconium, yttrium and aluminium acetylacetonates. Hot isostatic pressing has been performed for 1 h at 1130 and 1230 °C under 196 MPa using their powders. Two kinds of material are fabricated: (i) perfect ZrO_2 solid-solution ceramics and (ii) composites of ZrO_2 solid solution and α - Al_2O_3 . Their mechanical properties are examined, in connection with microstructures and *t/m* ZrO_2 ratios. Composites with a homogeneous dispersed α - Al_2O_3 derived from solid-solution ceramics result in a remarkable increase of strength.

1. Introduction

It has previously been reported [1] that in the system ZrO_2 – Al_2O_3 , metastable ZrO_2 solid solutions containing up to ~ 40 mol % Al_2O_3 were formed at low temperatures from amorphous materials prepared by the simultaneous hydrolysis of zirconium and aluminium alkoxides. In addition, the composition 75 mol % ZrO_2 –25 mol % Al_2O_3 powders were sintered at 1000–1150 °C under 196 MPa by using the hot isostatic pressing technique. The results showed that the ZrO_2 solid-solution ceramics consisting of a homogeneous microstructure with an average grain size of ~ 50 nm gave a very high fracture toughness of 23 MPa m^{1/2}. However, their strength was weak, in which the maximum value was 700 MPa. The purpose of the present study is to improve the strength of ZrO_2 solid-solution ceramics. Two kinds of material were fabricated by the addition of a small amount of Y_2O_3 : (i) perfect ZrO_2 solid-solution ceramics and (ii) composites of ZrO_2 solid solution and α - Al_2O_3 .

Doped ZrO_2 ceramics have traditionally been fabricated by sintering mixtures of ZrO_2 powders with the desired stabilizing oxide powders. This process generally results in the formation of inhomogeneous materials. It is therefore advantageous to produce the ceramics using specially prepared powders. The best known and most widely used preparation method has been the chemical reaction route, using for instance co-precipitation (e.g. [2]) and hydrolysis of alkoxides

(e.g. [3]); developments in this direction led to the production of highly reactive powders with controlled size and shape. The hydrolysis of acetylacetonates, because of the simpler process and the lower cost than alkoxides, is an effective method for the powder production.

2. Experimental procedure

Three acetylacetonates, $Zr(C_5H_7O_2)_4$, $Y(C_5H_7O_2)_3$ and $Al(C_5H_7O_2)_3$, were obtained commercially. They were dissolved in an excess of analytical-grade 2-propanol. The mixed solution was refluxed for 10 h at 82 °C and then hydrolysed by adding a large amount of aqueous ammonia (28 wt %) at room temperature. The temperature was slowly raised for ~ 1 h to 75 °C while the resulting suspension was stirred. The hydrolysis products of the various compositions, shown in Table I, were separated from the suspensions by centrifugation, washed five times in hot water and dried at 120 °C under reduced pressure. The powders obtained are termed starting powders A–F.

3. Results and discussion

3.1. Crystallization of metastable *t*- ZrO_2 solid solution

All starting powders were amorphous to X-rays. They were highly agglomerated and the primary particle

* To whom correspondence should be addressed.

TABLE I Chemical composition of starting powders, HIPing temperature and *t/m* ratio in materials

Starting powder	Composition		HIPing temperature (°C)	<i>t/m</i> ratio (%)
	ZrO ₂ /Y ₂ O ₃ /Al ₂ O ₃ (mol %)	Y ₂ O ₃ /(ZrO ₂ + Y ₂ O ₃) (mol % ratio)		
A	74.25/0.75/25	1.0	1130	47/53
			1230	24/76
B	73.50/1.50/25	2.0	1130	80/20
			1230	100/0
C	73.12/1.88/25	2.5	1130	100/0
			1230	100/0
D	72.75/2.25/25	3.0	1130	100/0
			1230	100/0
E	72.00/3.00/25	4.0	1130	100/0
			1230	100/0
F	71.25/3.75/25	5.0	1130	100/0
			1230	100/0

size could not be resolved by scanning electron microscopy (SEM); however, examination by transmission electron microscopy (TEM) showed primary particles of ~ 10 nm (Fig. 1).

Differential thermal analysis (DTA) was conducted in air at a heating rate of 10 °C min⁻¹; α-Al₂O₃ was used as the reference. Heated specimens, obtained from the DTA runs after cooling, were examined by

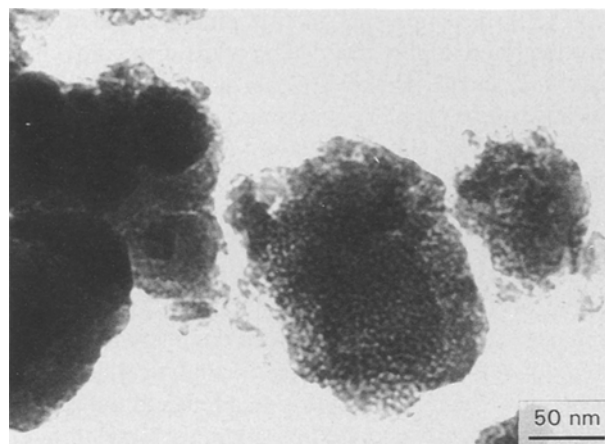


Figure 1 Transmission electron micrographs of starting powder D.

X-ray diffraction (XRD) using Ni-filtered CuK_α radiation. Exothermic peaks resulting from the crystallization of *t*-ZrO₂ solid solution were observed at ~ 780 to ~ 860 °C in all starting powders. Table II shows the phases identified for the specimens at various temperatures. No significant change in structure was recognized up to the temperatures of the exothermic peaks. The specimens heated at 860–1200 °C showed the *t*-ZrO₂ phase. Intermediate aluminas, such as γ- and θ-Al₂O₃, and α-Al₂O₃ were not confirmed through the heating process up to 1200 °C. The earlier paper dealing with the ZrO₂-Al₂O₃ system showed that *c*-ZrO₂ solid solutions crystallized at low temperatures and then transformed into solid solutions of *t*-ZrO₂ at higher temperatures [1]. The present results for materials containing a small amount of Y₂O₃ suggest that *t*-ZrO₂ solid solutions were formed from amorphous materials. Although no peaks were detected in the DTA, tetragonal-to-monoclinic ZrO₂ transformation occurred at ~ 1250 to ~ 1300 °C for powder A. Precipitates of α-Al₂O₃ from the solid solution were also observed above 1250 °C. The XRD intensities of the *m*-ZrO₂ phase and α-Al₂O₃ increased with increasing temperature. On the other hand, no phase transformation of ZrO₂ was recognized up to 1400 °C for powders D and F. The appearance of α-Al₂O₃ was shifted at higher temperatures with

TABLE II Phases identified for specimens quenched after heating to various temperatures

Starting powder	Phases identified ^a				
	800 °C	900–1200 °C	1250 °C	1300 °C	1400 °C
A	Amorphous	<i>t</i>	<i>t,m</i> α-Al ₂ O ₃	<i>t,m</i> α-Al ₂ O ₃	<i>m</i> α-Al ₂ O ₃
D	Amorphous	<i>t</i>	<i>t</i>	<i>t</i> α-Al ₂ O ₃	<i>t</i> α-Al ₂ O ₃
F	Amorphous	<i>t</i>	<i>t</i>	<i>t</i>	<i>t</i> α-Al ₂ O ₃

^a *t* = *t*-ZrO₂ phase, *m* = *m*-ZrO₂ phase.

increasing Y_2O_3 addition. When the powders were heated at $1400^\circ C$, the specimens were the mixtures of the $m-ZrO_2$ phase and $\alpha-Al_2O_3$ for powder A and of the $t-ZrO_2$ phase and $\alpha-Al_2O_3$ for D and F.

3.2. Sintering

Calcined powders consisting of the $t-ZrO_2$ phase were prepared by heating for 1 h at $1000^\circ C$. Before hot isostatic pressing, they were pressed into pellets at 196 MPa and then isostatically cold-pressed at 392 MPa. The green compacts covered with BN powders were sealed in a Pyrex glass tube under vacuum. Hot isostatic pressing experiments were performed for 1 h at 1130 and $1230^\circ C$ under 196 MPa using Ar gas as the pressure-transmitting medium. After the sintered materials were cut with a diamond saw, they were lapped with a diamond powder (nominal size 1–2 μm). The contents of $t-ZrO_2$ by vol % total ZrO_2 [4, 5] and $\alpha-Al_2O_3$ were measured by the X-ray technique on the fracture surfaces. The material of well-precipitated $\alpha-Al_2O_3$ was prepared by sintering powder A in air for 3 h at $1700^\circ C$. The fractional precipitation was determined from the ratio of the intensity using the (113) line. No presence of intermediate alumina and $\alpha-Al_2O_3$ was observed in materials fabricated at $1130^\circ C$; as will be described, they consisted of either mixtures of t - and $m-ZrO_2$ phases or only $t-ZrO_2$ phase. The results indicate that perfect ZrO_2 solid-solution ceramics were fabricated. On the other hand, materials fabricated at $1230^\circ C$ contained $\alpha-Al_2O_3$. Fig. 2 shows the fraction of $\alpha-Al_2O_3$ as a function of Y_2O_3 addition. The fraction decreased with increasing Y_2O_3 addition; in particular, it dropped sharply between 1.88 and 3 mol % Y_2O_3 .

Composites of ZrO_2 solid solution and $\alpha-Al_2O_3$, in which their contents could be controlled by the

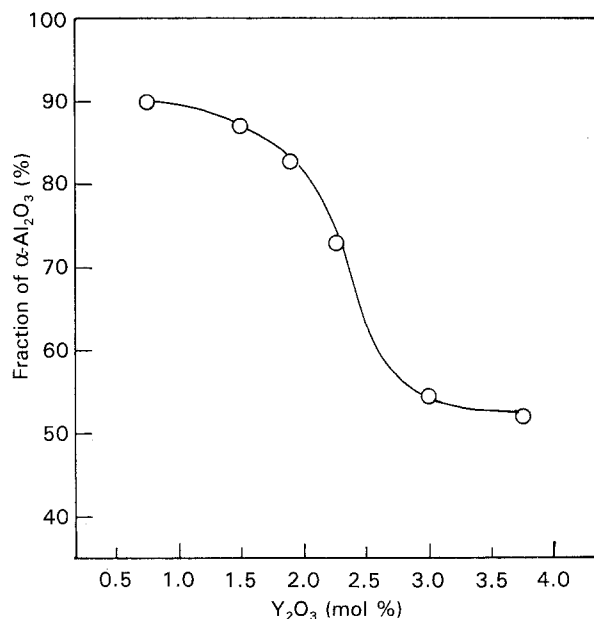


Figure 2 Fraction of $\alpha-Al_2O_3$ in composites as a function of Y_2O_3 addition.

* Hot isostatic pressing was performed at $1180^\circ C$. A similar curve, showing $\sim 25\%$ less fraction in each material than that at $1230^\circ C$, was obtained.

amount of Y_2O_3 addition and the sintering temperature*, could be easily fabricated. The microstructure was characterized by SEM. Fig. 3a shows the SEM (secondary electron image) photograph for the fracture surface of the dense solid-solution ceramics from powder D. The grain size was measured directly by SEM. The average grain size was $\sim 0.1 \mu m$ in all solid-solution ceramics. The $\alpha-Al_2O_3$ grains in composites could not be clearly resolved by the observation; however, the presence of homogeneous dispersed $\alpha-Al_2O_3$ grains was proved by back-scattered electron imaging of the polished and thermally etched surface (Fig. 3b). Intergranular $\alpha-Al_2O_3$ of $\sim 0.12 \mu m$ size was observed regardless of the starting composition.

The proportion of the t - and $m-ZrO_2$ phases is shown in Table I. The $m-ZrO_2$ phase was present in the solid-solution ceramics from powders A and B and in the composite from powder A. Above 1.88 mol % Y_2O_3 addition both materials consisted of the $t-ZrO_2$ phase. The absence of the $m-ZrO_2$ phase in the composite from powder B might be explained in terms of the increase of the Y_2O_3 concentration in ZrO_2 , as a result of the precipitation of $\alpha-Al_2O_3$. Bulk densities were verified by the Archimedes method (Fig. 4). The

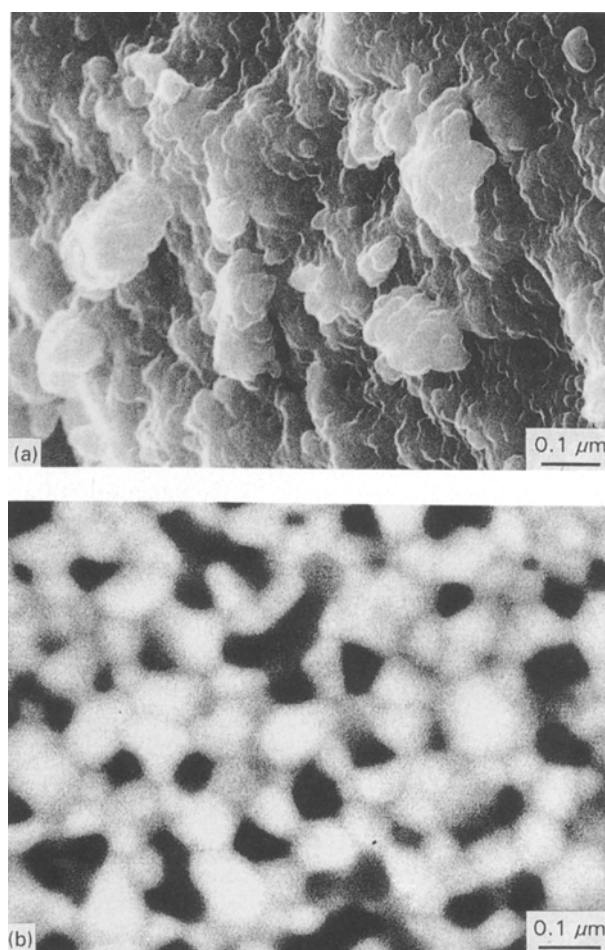


Figure 3 Scanning electron micrographs for (a) secondary electron image of solid-solution ceramics and (b) back-scattered electron image of composite fabricated from powder D. Black grains in the composite represent $\alpha-Al_2O_3$.

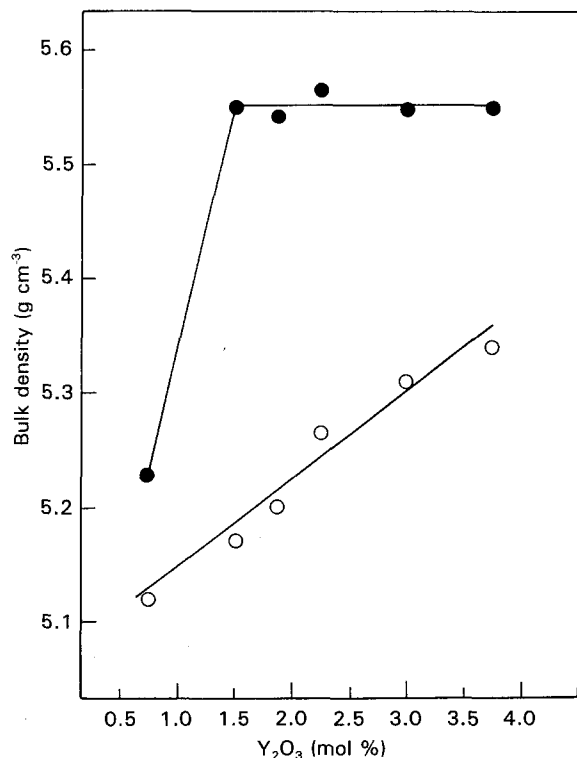


Figure 4 Bulk densities of (○) solid-solution ceramics and (●) composites as a function of Y₂O₃ addition.

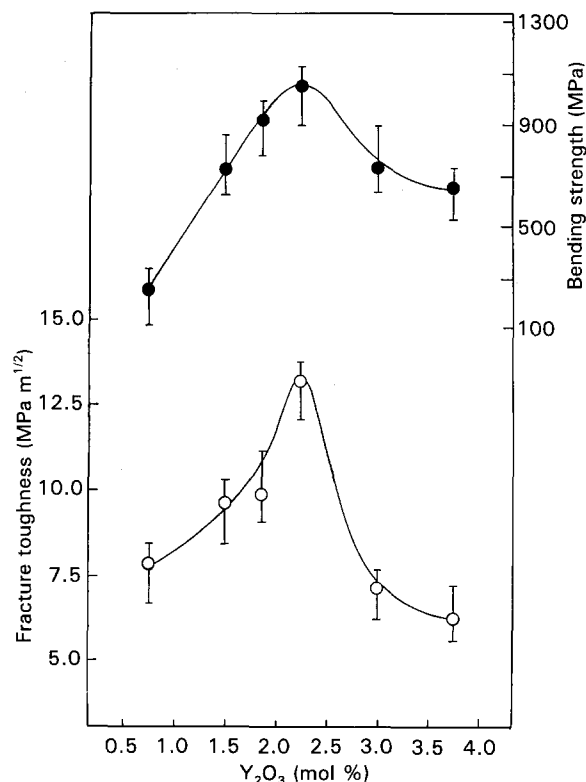


Figure 5 (○) Fracture toughness and (●) bending strength of solid-solution ceramics as a function of Y₂O₃ addition.

solid-solution ceramics increased linearly in density with increasing Y₂O₃ addition. The bulk densities of the composites increased rapidly between 0.75 and 1.5 mol % Y₂O₃ and attained a constant value ($\sim 5.55 \text{ g cm}^{-3}$) above 1.5 mol % Y₂O₃ addition. The theoretical densities of α -Al₂O₃, *t*-ZrO₂ and *m*-ZrO₂ are 3.987, 6.097 and 5.840 g cm⁻³, respectively [6]. Accordingly, the lower density of the composite with 0.75 mol % Y₂O₃ can be attributed to the presence of large amounts of α -Al₂O₃ and *m*-ZrO₂.

3.3. Mechanical properties

K_{Ic} measurements were made by the indentation fracture (IF) technique [7, 8] with 490 N Vickers load. The samples (3 mm × 20 mm × 3 mm) were subjected to the three-point bending strength test with a 16 mm span and a crosshead speed of 0.5 mm min⁻¹. Fig. 5 shows the fracture toughness and bending strength of the solid-solution ceramics as a function of Y₂O₃ addition. Curves with similar features were obtained for both of them. The maximum values of 13.2 MPa m^{1/2} and 1045 MPa for fracture toughness and strength, respectively, were achieved in the solid-solution ceramics with 2.25 mol % Y₂O₃. The strength was a much higher value than that of the solid-solution ceramics in the system ZrO₂-Al₂O₃. However, K_{Ic} gave a lower value. The tetragonal and monoclinic ZrO₂ particles enhance the toughness by creating a "stress-induced" transformation [9, 10] and by extending "pre-existing" microcracks [11, 12], respectively. The solid-solution ceramics in the binary system contained an *m*-ZrO₂ phase of 30–50 % [1]. The most highly toughened ceramics in the present study consisted of the *t*-ZrO₂ phase. The tetragonal-

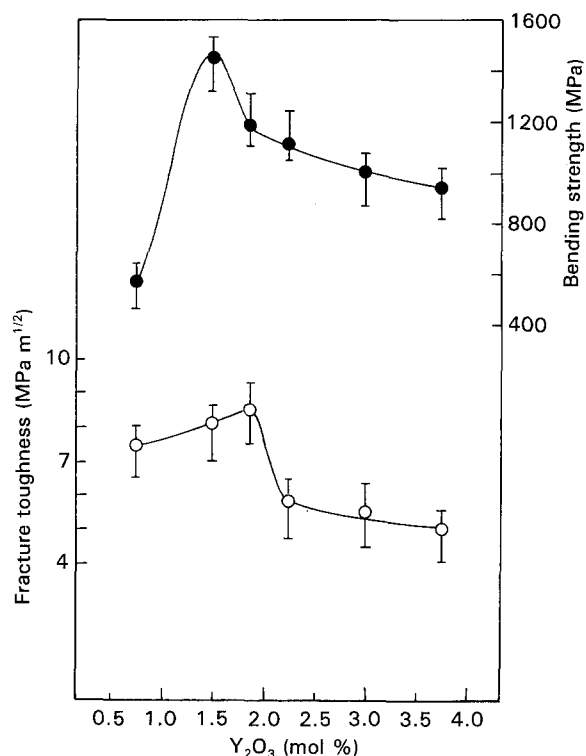


Figure 6 (○) Fracture toughness and (●) bending strength of composites as a function of Y₂O₃ addition.

to-monoclinic ZrO₂ transformation depends on the critical size of particles (e.g. [13]). The decrease of the K_{Ic} value must be due to stable *t*-ZrO₂ particles below the critical size being hard to transform by Y₂O₃ addition [14]. Excellent strength (1445 MPa) and high fracture toughness (8.5 MPa m^{1/2}) were obtained in the composites with 1.5 and 2 mol % Y₂O₃, respectively

(Fig. 6). The composites with a homogeneous dispersed α -Al₂O₃ derived from the solid-solution ceramics resulted in a remarkable improvement of strength. The composition dependence of the mechanical properties of toughened ZrO₂-Y₂O₃ ceramics has been widely studied (e.g. [15]). Both fracture toughness and strength are known to give a maximum value at a particular composition: 2 mol% Y₂O₃ for the former and either 2.5 or 3 mol% Y₂O₃ for the latter. The data for the composites, as can be seen from the composition ratios in Table I, agreed with these results.

References

1. S. INAMURA, H. MIYAMOTO, Y. IMAIDA, M. TAKAGAWA, K. HIROTA and O. YAMAGUCHI, *J. Mater. Sci.* in press.
2. A. H. HEUER, N. CLAUSSEN, W. H. KRIVEN and M. RÜHLE, *J. Amer. Ceram. Soc.* **65** (1982) 642.
3. P. F. BECHER, *ibid.* **64** (1981) 37.
4. R. C. GARVIE and P. S. NICHOLSON, *ibid.* **55** (1972) 303.
5. H. TORAYA, M. YOSHIMURA and S. SOMIYA, *ibid.* **67** (1984) C-119.
6. S. HORI, M. YOSHIMURA and S. SOMIYA, *J. Mater. Sci. Lett.* **4** (1985) 413.
7. A. G. EVANS and E. A. CHARLES, *J. Amer. Ceram. Soc.* **59** (1976) 311.
8. K. NIIHARA, A. NAKAHIRA and T. HIRAI, *ibid.* **67** (1984) C-13.
9. R. McMECKING and A. G. EVANS, *ibid.* **65** (1982) 242.
10. B. BUDIANSKY, J. W. HUTCHINSON and J. C. LAMBROPOULOS, *Int. J. Solids Struct.* **19** (1983) 337.
11. A. G. EVANS and K. T. FABER, *J. Amer. Ceram. Soc.* **64** (1981) 394.
12. *Idem*, *ibid.* **67** (1984) 255.
13. R. STEVENS and P. A. EVANS, *Br. Ceram. Trans. J.* **83** (1984) 23.
14. F. F. LANGE, *J. Mater. Sci.* **17** (1982) 247.
15. J. WANG, M. RAINFORTH and R. STEVENS, *Br. Ceram. Trans. J.* **88** (1989) 1.

Received 29 July 1993

and accepted 19 January 1994